Initial navigation alignment of optical instruments on GOES-R

A31D-0063

Peter J. Isaacson[1], Frank J. DeLuccia[1], Alan D. Reth[2], David A. Igli[3], Delano R. Carter[4]

[1]The Aerospace Corporation [2]Chesapeake Aerospace LLC/NASA GSFC [3]ASRC Federal Technical Services LLC/NASA GSFC [4]Thearality, Inc./NASA GSFC

Abstract

Post-launch alignment errors for the Advanced Baseline Imager (ABI) and Geospatial Lightning Mapper (GLM) on GOES-R may be too large for the image navigation and registration (INR) processing algorithms to function without an initial adjustment to calibration parameters. We present an approach that leverages a combination of user-selected image-to-image tie points and image correlation algorithms to estimate this initial launch-induced offset and calculate adjustments to the Line of Sight Motion Compensation (LMC) parameters. We also present an approach to generate synthetic test images, to which shifts and rotations of known magnitude are applied. Results of applying the initial alignment tools to a subset of these synthetic test images are presented. The results for both ABI and GLM are within the specifications established for these tools, and indicate that application of these tools during the post-launch test (PLT) phase of GOES-R operations will enable the automated INR algorithms for both instruments to function as intended.

Introduction

The GOES-R satellite is the first in NOAA's next-generation series of geostationary weather satellites [1]. In addition to a number of space weather sensors, it will carry two principal optical earth-observing instruments, the ABI [2] and the GLM [3]. During launch, the alignment of these optical instruments is anticipated to shift from that measured during pre-launch characterization. While both instruments have image navigation and registration (INR) processing algorithms to enable automated geolocation of the collected data, the launch-induced misalignment may be too large for these algorithms to function without an initial adjustment to calibration parameters. Adjustments to the LMC parameters will be estimated on orbit during PLT.

We have developed approaches to estimate the initial alignment errors for both ABI and GLM image products. Our approaches involve comparison of ABI and GLM images collected during PLT to a set of reference ("truth") images using custom image processing tools and other software (referred to as the INR Performance Assessment Tool Set, or "IPATS") being developed for other INR assessments of ABI and GLM data [4, see below]. In this work we present an overview of the tools developed to perform the initial alignment assessment required to update the LMC parameters. We also present our approach to generate synthetic test data as well as a subset of the results of applying the initial alignment tools to the synthetic test data.

IPATS/IPSE Overview

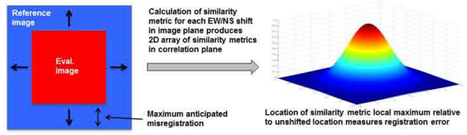

Figure 1: Cross correlation approach to INR evaluation using image registration. The evaluation image is shifted within the reference image, and the misregistration is determined from the offset between the similarity metric maximum and the unshifted location.

The Image Navigation and Registration (INR) Performance Assessment Tool Set (IPATS) was developed by the GOES-R Flight Project to facilitate evaluation of INR performance of the ABI and the GLM. IPATS is comprised of two related tools, the Image Pair Selector and Evaluator (IPSE) and the Output Database Analysis Tool (ODAT). IPSE is a C++-based tool that, at its most basic level, determines the misregistration in pixels between two input images. IPSE has the capability to perform this analysis using a variety of image correlation algorithms and pre-processing optimizations [4]. The current default analysis flow leverages the Normalized Cross Correlation algorithm [5]. IPSE supports a variety of INR metrics, both relative and absolute. For relative assessments, images are compared to other images of the same type (e.g., ABI image to ABI image). For absolute assessments, images are compared to truth images. In the case of ABI, the truth images are Landsat 8-based reference image "chips" [4]. In the case of GLM, the truth image is a navigated ABI image [4, 6]. In the application presented here, both absolute (ABI initial alignment) and relative (GLM initial alignment) assessments are leveraged. The ODAT is used to convert the output database to comma separated value (CSV) format for ingestion into the initial alignment post-processing tools.

Initial Alignment Processing Flow (IAPF)

In both the ABI and GLM cases, the initial step requires a user to select image-to-image tie points (also known as control points). These tie points facilitate a rough estimation of the gross offset between the evaluated image and the reference image. Application of this initial offset estimate yields an answer sufficiently close for refinement of the calculated offset with IPSE. Note that this tie point step is not imposed fundamentally by IPSE, which can theoretically support arbitrarily large offsets, but rather by the reference images. Excessively large offsets between the evaluated and truth image would cause the reference and evaluated image to not share common geographic coverage, leading to a failure of the correlation algorithm. In the GLM case, the ABI and GLM images are resampled to a common resolution, both to support image-to-image tie point selection and to address the irregular ground sample distance in fixed grid coordinates of the GLM background images, which result from the GLM background images having uniform pixel size in focal plane coordinates rather than in instantaneous field of view (IFOV) [3, 6].

A summary of the processing steps performed by the initial alignment tool is:

1. **For GLM input images, resample GLM and associated ABI images (closest temporal and spectral collects) to common angular resolution, e.g. 56 µrad.**
2. **For an input set of images (e.g., acquired over a 24 hour period), pick a representative image (likely local noon) to generate tie points. Pick tie points.**
3. **Determine offset based on tie points.**
4. **Run IPSE for all images in set, accounting for initial offset from 3. Reference image is Landsat chip (ABI), or associated ABI image (GLM). Individual misregistrations are determined for each Landsat chip (ABI) or pre-defined subimage region (based on a defined pattern of evaluation locations) (GLM).**
5. **Convert IPSE output to CSV format.**
6. **Run initial alignment post-processing (rigid rotation) to determine least squares shift and rotation for full image from set of local misregistrations.**

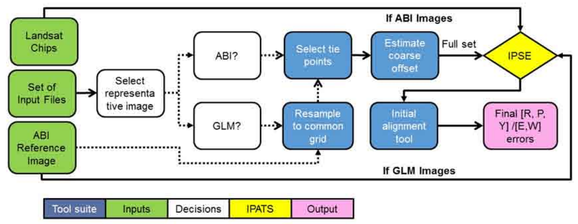

Figure 2: Simplified illustration of initial alignment tool processing flow. The ABI and GLM cases differ in the common grid resampling and the reference images used (Landsat chips for ABI, ABI reference image for GLM).

Least Squares Optimization Approach

Two least squares minimization approaches were developed to determine optimized shift and rotation parameters for the rigid rotation algorithm (see below).The first approach relies on singular value decomposition [7], and the second is an iterative approach using the MPFIT algorithm [8]. Since the singular value decomposition approach can be found in [7] and requires only simplification to the 2-D case and proper definition of variables to implement, we present details here only for the MPFIT approach.

Assume IPSE correlations are performed at a set of points (x,y). Let Warp Points (WP) be the adjusted points after applying the IPSE-determined offsets $(x+\Delta x, y+\Delta y)$. Model Warp Pts. (**MWP**) is defined by applying the optimized shift and rotation to the (x, y) correlation centers (**A**):

$$\boldsymbol{MWP} = \boldsymbol{RA} + t \quad (1)$$

$\boldsymbol{R}$ and t are defined as:

$\boldsymbol{R} = \begin{bmatrix} \cos\theta & -\sin\theta \\ \sin\theta & \cos\theta \end{bmatrix}, t = \begin{bmatrix} t_x \\ t_y \end{bmatrix}$. Thus, the least squares optimization has three free parameters (the rotation angle, the x component of the translation, and the y component of the translation).

The error to be minimized is defined as a Euclidean distance:

$E = \sqrt{(MWP_x - WP_x)^2 + \left(MWP_y - WP_y\right)^2}$ (2). The IDL package MPFIT is used to obtain optimized values for θ and t such that E is minimized.

Rigid Rotation Algorithm

Individual misregistrations (Δx, Δy) are used to determine an optimized global offset and rotation. The optimized shift and rotation is determined via a least squares minimization of the error between the "point cloud" of local misregistrations ($x+\Delta x$, $y+\Delta y$) and the "point cloud" of locations after applying the optimized offset and rotation. We use a scale-invariant shift and rotation approach where the free parameters are shift (x,y) and rotation (z), rather than an affine transformation that would also allow scaling and shearing, since it more closely models the physics of the launch-induced misalignment (shift and rotation only).

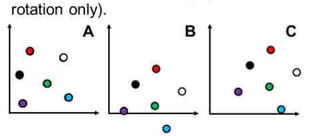

Figure 3: Illustration of rigid rotation concept. From left to right: Original point cloud (A), pt. cloud with 30° rotation (B), pt. cloud with 30° rotation and positive x and y shift (C).

Synthetic Test Image Generation

To evaluate the performance of the initial alignment tools, a series of images with known shifts and rotations applied were required. Rotations and shifts were applied with the Matlab utilities griddata (irregular grid interpolation) and fraccircshift [9]. Griddata interpolates an input image grid with coordinates points (X_o, Y_o) to a new output grid with points (X, Y). The grids can be regular or irregular. The output grid (X, Y) is determined by the application of a rotation matrix (see above) to (X_o, Y_o) after transforming from pixel coordinates $(0…n, 0..n)$ to Cartesian coordinates $(-n/2…n/2, -n/2…n/2)$ by subtracting the center pixel coordinate $(n/2, n/2)$. Fraccircshift applies a circular shift to the image of $(\Delta x, \Delta y)$, where the shifts can be fractional pixels. Synthetic test images were generated to span the expected error budget (#pixels) in each axis (roll, pitch, yaw) for both ABI and GLM.

Correlation Results for Test Images

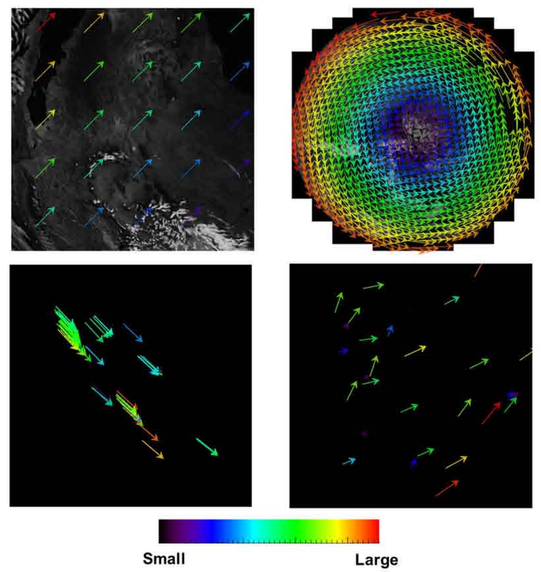

Figure 4: Illustration of $(\Delta x,\Delta y)$ offsets derived from image correlation (IPSE) analyses. These local offsets are the inputs to the least squares optimization of the rigid rotation (see above). Images illustrate (***UL***) equal magnitude positive shift/rotation in all three axes, small image, autocorrelation (***UR***) positive rotation only (yaw axis), autocorrelation, ABI full disk (***LL***) equal magnitude positive shift/rotation in all three axes (IPSE analysis of ABI proxy image against Landsat chips), ABI full disk (***LR***) GLM case, equal magnitude shift/rotation in all three axes (IPSE analysis of rotated/shifted/rebinned proxy GLM image against rebinned ABI reference). Color indicates the magnitude of the offset, but does NOT have the same scale in all images.

Requirements Formulation

The line-of-sight uncertainty (accuracy) requirement for the initial alignment tool is defined in fixed grid angles (east-west, north-south) rather than per-axis [6]. The east-west and north-south uncertainties are derived from a root sum of squares of the pitch and yaw errors, roll and yaw errors, respectively. The conversion is as follows, with the yaw contribution being defined at the edge of the instrument field of regard (FOV_{ABI} = 11°, FOV_{GLM} = 8°).

$$s_{EW} = \sqrt{{s_{pitch}}^2 + \left(FOV° * \frac{\pi}{180°} * s_{yaw}\right)^2} \quad (3)$$

$$s_{NS} = \sqrt{{s_{roll}}^2 + \left(FOV° * \frac{\pi}{180°} * s_{yaw}\right)^2} \quad (4)$$

Example Results (Synthetic Test Data)

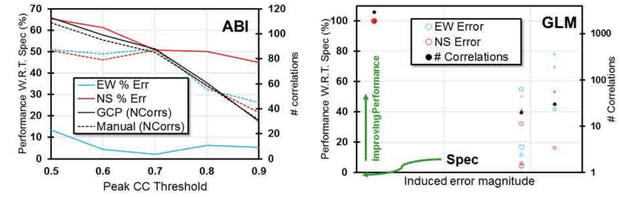

Figure 5: Plots of tool performance w.r.t requirements on synthetic ABI (**L**) and GLM (**R**) images. In both cases, positive performance % indicates greater margin w.r.t the specification (i.e., a value of 100% indicates perfect accuracy, and negative values would indicate accuracy below the specification). The ABI plot shows two cases, where the same image was evaluated with control point-derived (solid) and ideal (dashed) initial offsets (see IAPF section). Performance is illustrated over a range of correlation coefficient threshold values, which defines the minimum correlation quality for a point to be included in the least squares analysis. Accuracy decreases with increasing peak CC, largely driven by the decreasing sample size. The GLM plot shows three test images with different synthetic errors (the left-most point is the null case with no error applied). This evaluation was done with a peak CC of 0.5. Different y points for the same x indicate different tie-point-derived offset errors, indicated by the sizes of the points (see IAPF section). The right-most set of points has improved performance, likely due to the larger # of correlations. The reason for the image with increased initial error having more surviving correlations is the subject of ongoing research. In all cases illustrated, the performance exceeds the specification with a comfortable margin.

Discussion & Conclusions

- The tool exhibits sensitivity to the accuracy of the image-to-image tie point selection, indicating that significant care must be taken during this step.
- All but the most extreme error cases (not shown) are within spec with comfortable margin.
- More extreme cases will require more careful tie point selection.
- Results indicate that application of these tools during PLT will yield a positive outcome in which the automated INR algorithms will be applied successfully.

References

[1] Krimchansky, Alexander, et al. (2004), *Remote Sensing*, Proc. SPIE 5570, doi: 10.1117/12.565281. [2] Schmit, Timothy J., et al. (2005), *Bulletin of the American Meteorological Society* **86.8** 1079, doi: 10.1175/BAMS-86-8-1079. [3] Goodman, S., et al. (2013), Atmospheric Research, **125-126**, doi: 10.1016/j.atmosres.2013.01.006 . [4] De Luccia, Frank J., et al. (2016), *SPIE Asia-Pacific Remote Sensing*, Proc. SPIE 9881, doi: 10.1117/12.2229059. [5] Lewis, J. P. (1995), *Vision* interface, **10**. [6] Product Definition and Users' Guide (PUG) Volume 3: Level 1B Products for Geostationary Operational Environmental Satellite R Series (GOES-R) Core Ground Segment, Revision D, 13 May 2015, http://www.goes-r.gov/users/docs/PUG-L1b-vol3.pdf. [7] Sorkine, Olga. (2009), *Technical notes* **120.3**. [8] Markwardt, Craig B. (2009), *Instrumentation and Methods for Astrophysics*, arXiv:0902.2850. [9] Available from the Matlab File Exchange at https://www.mathworks.com/matlabcentral/fileexchange/45950-fraccircshift.

Acknowledgements

The authors would like to acknowledge the support of the GOES-R Flight Program.

Contact Information

Peter J. Isaaccson
The Aerospace Corporation
MS CH3-240
14301 SullyField Circle, Unit C
Chantilly VA 20151-1409

(571)-307-3882
Peter.J.Isaacson@aero.org

AEROSPACE
Assuring Mission Success